Unusual Low Reactivity of the Water Oxidase in Redox State S_3 toward Exogenous Reductants. Analysis of the NH_2OH- and NH_2NH_2-Induced Modifications of Flash-Induced Oxygen Evolution in Isolated Spinach Thylakoids†

J. Messinger, U. Wacker, and G. Renger*

Max-Volmer-Institut für Biophysikalische und Physikalische Chemie, Technische Universität Berlin, Strasse des 17. Juni 135, W-1000 Berlin 12, FRG

Received February 28, 1991; Revised Manuscript Received May 13, 1991

ABSTRACT: The effect of redox-active amines NH_2R (R = OH or NH_2) on the period-four oscillation pattern of oxygen evolution has been analyzed in isolated spinach thylakoids as a function of the redox state S_i (i = 0, ..., 3) of the water oxidase. The following results were obtained: (a) In dark-adapted samples with a highly populated S_1 state, NH_2R leads via a dark reaction sequence to the formal redox state "S_{-1}"; (b) the reaction mechanism is different between the NH_2R species; NH_2OH acts as a one-electron donor, whereas NH_2NH_2 mainly functions as a two-electron donor, regardless of the interacting redox state S_i (i = 0, ..., 3). For NH_2NH_2, the modified oxygen oscillation patterns strictly depend upon the initial ratio $[S_0(0)]/[S_1(0)]$ before the addition of the reductant; while due to kinetic reasons, for NH_2OH this dependence largely disappears after a short transient period. (c) The existence of the recently postulated formal redox state "S_{-2}" is confirmed not only in the presence of NH_2NH_2 [Renger, G., Messinger, J., & Hanssum, B. (1990) in *Current Research in Photosynthesis* (Baltscheffsky, M., Ed.) Vol. 1, pp 845–848, Kluwer, Dordrecht] but also in the presence of NH_2OH. (d) Activation energies, E_A, of 50 kJ/mol were determined for the NH_2R-induced reduction processes that alter the oxygen oscillation pattern from dark-adapted thylakoids. (e) Although marked differences exist between NH_2OH and NH_2NH_2 in terms of the reduction mechanism and efficiency (which is about 20-fold in favor of NH_2OH), both NH_2R species exhibit the same order of rate constants as a function of the redox state S_i in the nonperturbed water oxidase:

$$k_{NH_2R}(S_0) > k_{NH_2R}(S_1) \ll k_{NH_2R}(S_2) \gg k_{NH_2R}(S_3)$$

The large difference between S_2 and S_3 in their reactivity toward NH_2R is interpreted to indicate that a significant change in the electronic configuration and nuclear geometry occurs during the $S_2 \rightarrow S_3$ transition that makes the S_3 state much less susceptible to NH_2R. The implications of these findings are discussed with special emphasis on the possibility of complexed peroxide formation in redox state S_3 postulated previously on the basis of theoretical considerations [Renger, G. (1978) in *Photosynthetic Water Oxidation* (Metzner, H., Ed.) pp 229–248, Academic Press, London].

Photosynthetic water oxidation to dioxygen that is accompanied by proton release into the thylakoid lumen takes place within the PS II[1] complex via a sequence of univalent redox steps. After the accumulation of four oxidizing redox equivalents (holes) in a manganese-containing unit the product, O_2, is released. It is not yet clear whether this hole storage unit, HSU(Mn), also comprises the water-oxidizing site (WOS) [for a discussion, see Wydrzynski et al. (1985), Renger et al. (1990b), and Renger and Wydrzynski (1991)]. The reaction sequence referred to as the Kok cycle (Kok et al., 1970) is energetically driven by $P680^+$ as the oxidant, formed during the primary step of charge separation within the reaction center. A redox component, Y_Z, recently identified in *Synechocystis* sp. PCC 6803 as Tyr-161 of polypeptide D1 (Debus et al., 1988a; Metz et al., 1989) of the PS II apoprotein, acts as an intermediate electron carrier between PS II and the manganese-containing hole storage unit. The redox state of the water oxidase is symbolized by S_i, where i indicates the number of accumulated oxidizing equivalents. The kinetics of the elementary reactions in the overall sequence of PS II have been resolved in great detail by various spectroscopic techniques [for recent reviews, see Babcock (1987), Renger (1987a), Rutherford (1989), Hansson and Wydrzynski (1990), and Renger and Wydrzynski (1991)]. A scheme for the functional organization of photosynthetic water oxidation is summarized in Figure 1.

In addition to the main electron transport pathway, referred to as the "active branch" of the PS II donor site, other internal redox components can interfere with the reaction pattern. The polypeptide D2 of the PS II apoprotein also contains a redox-active tyrosine residue, Y_D (Tyr-160 in *Synechocystis* sp. PCC 6803; Debus et al., 1988b; Vermaas et al., 1988). This tyrosine, however, does not participate in the main pathway (and may be part of an "inactive branch" of the PS II donor

† The financial support by Deutsche Forschungsgemeinschaft (Re-354/12-1) and Fonds der Chemischen Industrie is gratefully acknowledged.

* To whom correspondence should be addressed.

[1] Abbreviations: C_{II}, proposed one or two electron acceptor for NH_2R in binding site X; D1, D2, polypeptides of photosystem II core; HEPES, *N*-(2-hydroxyethyl)piperazine-*N'*-2-ethanesulfonic acid; HSU(Mn); manganese-containing hole storage unit of photosystem II water oxidase; NH_2R, R = NH_2, hydrazine or R = OH, hydroxylamine; PS II, photosystem II; P680, primary electron donor in PS II; S_i, redox state i of the water oxidase; Tris, tris(hydroxymethyl)aminomethane; WOS, water-oxidizing site; Y_D, redox-active tyrosine of polypeptide D2; Y_Z, redox-active tyrosine of polypeptide D1 that acts as electron donor to $P680^+$; X, proposed binding site for NH_2R in the water oxidase.

0006-2960/91/0430-7852$02.50/0

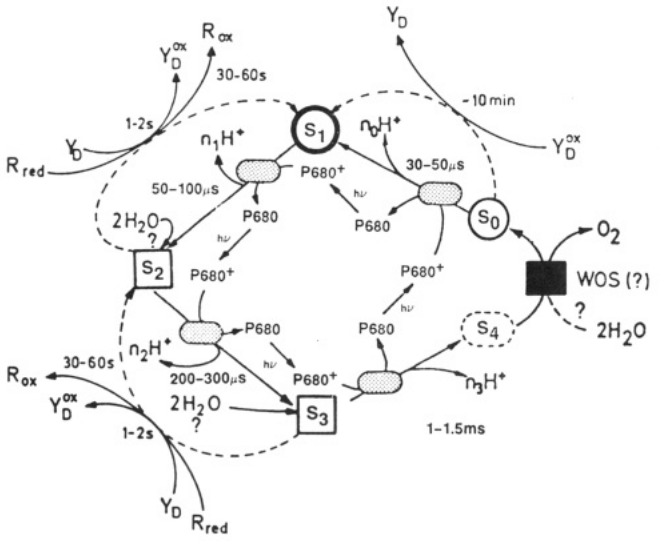

FIGURE 1: Functional scheme of photosynthetic water oxidation via a four-step univalent redox sequence energetically driven by photooxidized $P680^+$. The stabilities of the different redox states of the hole storage unit HSU(Mn) are symbolized by a thick circle for the dark stable state S_1 and by a thin circle for the metastable S_0. The transient redox states S_2 and S_3 are symbolized by squares, while the kinetically undetectable S_4 state is characterized by a dashed oval. The possibility of a separate water-oxidizing site is symbolized by WOS with a question mark. Likewise, the unresolved stage(s) of substrate water entry into the redox cycle is (are) also symbolized by question marks. The electron transfer times of the multiphasic $P680^+$ reduction are omitted; those for the $S_i \rightarrow S_{i+1}$ transition with Y_Z^{ox} as oxidant are depicted at the arrows of these reactions (the redox couple Y_Z^{ox}/Y_Z is symbolized by a grey oval). R represents all other endogenous reductants (e.g. Q_B^- at the acceptor side) that are able to reduce S_2 and S_3 (for the sake of simplicity only univalent reactions are shown); n_i represents the number of protons that are released during an individual redox transition $S_i \rightarrow S_{i+1}$. For further details, see the text.

side), but it can interact with the different redox states of HSU(Mn). In its reduced form, Y_D causes the dissipation of one oxidizing equivalent, if HSU(Mn) attains either the redox state S_2 or S_3, while in its oxidized form Y_D^{ox}, it can abstract one electron from the S_0 state leading to S_1 (Styring & Rutherford, 1988). On the other hand, the redox states S_2 and S_3 also slowly decay to S_1 via back-reactions with the acceptor side, probably involving Y_Z and P680 as intermediates, as has been inferred from delayed light emission (Rutherford & Inoue, 1983) and thermoluminescence measurements (Rutherford et al., 1984). In addition, interaction with other endogenous donors may be possible as well. In view of this complexity, the slow reduction of S_2 and S_3 by endogenous electron donors other than Y_D will be simply symbolized in Figure 1 by interaction with R_{red} in its reduced and R_{ox} in its oxidized form.

The detailed scheme of Figure 1 does not provide information on the actual chemical mechanism of water oxidation. In order to resolve this problem, the electronic configuration and the nuclear geometry of the HSU(Mn) in each individual redox state, S_i, and, if there exists a separate site, also of WOS (see Figure 1) need to be known. Despite recent progress, this goal is far from being reached [for a recent discussion, see Renger and Wydrzynski (1991)]. Among different approaches to address this problem, specific exogenous substances can be used as a powerful tool to modify the reaction pattern in a very selective way. Two types of agents are especially suited for this purpose: (a) ADRY-type substances (Renger, 1972), which cause a selective decay of S_2 and S_3 without affecting the electron transfer from Y_Z to $P680^+$ (Renger et al., 1989), and (b) reductants such as NH_2OH and NH_2NH_2, which induce a shift of the oscillation pattern in the flash-induced yield of oxygen evolution in thylakoids (Bouges, 1971; Kok & Velthuys, 1977) and PS II membrane fragments (Hanssum & Renger, 1987).

The latter effect has often been used in attempts to manipulate the S_i state population in a definite manner. It was assumed that NH_2OH directly reduces manganese of the HSU(Mn) (Saygin & Witt, 1987; Beck & Brudvig, 1987). Apart from the fact that the proposal of direct two-electron reduction of manganese in S_1 with NH_2OH is at variance with recent XANES data (Guiles et al., 1990a), the reaction pattern induced by this substance appears to be much more complex than a simple dissipation of two oxidizing redox equivalents (Bouges, 1971; Hanssum & Renger, 1985; Lavergne, 1989). Furthermore, the oscillation pattern of the oxygen yield per flash observed in NH_2NH_2-treated samples was shown to depend on the population of S_0 and S_1 prior to NH_2NH_2 addition. On the basis of this finding, NH_2NH_2 was inferred to introduce a surplus of two electrons into PS II that can be described by formal "S_{-1}" and "S_{-2}" states arising from S_1 and S_0, respectively (Renger et al., 1990b; Messinger & Renger, 1990a). The nature of these states is as yet unresolved.

In the present study, comparative measurements were performed with NH_2OH and NH_2NH_2 in order to analyze the reaction sequences and the mechanism leading to a change of the total redox equivalents that can interfere with the HSU(Mn).

Materials and Methods

Thylakoids were prepared from market spinach according to the procedure described by Winget et al. (1965). In these samples, the redox state of Y_D can be properly manipulated as described recently (Messinger & Renger, 1990a).

The flash-induced O_2 oscillation patterns were measured with a modified Joliot-type electrode (Joliot, 1972) that keeps the temperature of the buffer reservoir and the electrode constant within ±0.3 °C. The measurements of this study were performed at an electrode temperature of 7 °C. Our Joliot-type electrode does not allow rapid injection and mixing of the sample with exogenous substances. Therefore, the following procedure was used: 80 μL of the sample containing thylakoids in redox state $Y_D^{ox}S_1$, 0.3 M mannitol, 20 mM $CaCl_2$, 10 mM $MgCl_2$, and 50 mM Hepes/NaOH, pH 7.2, were illuminated with one, two, or three flashes in order to populate the redox states $Y_D^{ox}S_2$, $Y_D^{ox}S_3$, and $Y_D^{ox}S_0$, respectively. Immediately after the flash(es), 20 μL of buffer with or without NH_2OH or NH_2NH_2 was added, leading to a final chlorophyll concentration of 1 mg/mL and the concentration of NH_2OH (NH_2NH_2) given in the figure legends. The samples were kept on ice for the desired dark time. After this treatment, 10 μL of the suspension were rapidly transferred in the dark to the Joliot-type electrode, and the polarization (-750 mV) was switched on about 20 s before the measurement. The time required for this manipulation was about 1 min so that the total dark incubation of the state $Y_D^{ox}S_i$ is given by the storage time in the ice bath plus the time gap of 1 min between sample transfer and measurement. Alternatively, measurements were performed as a function of NH_2OH (NH_2NH_2) concentration at a constant dark incubation time of 1 min.

The deconvolution of the measured oxygen yield data into the S_i-state populations was performed with a fit program based on the formula

$$\mathbf{S}_n = \mathbf{K} \cdot \mathbf{S}_{n-1} \qquad (1a)$$

and

$$Y_n = (1 - \alpha)[S_3]_{n-1} + \beta[S_2]_{n-1} \quad (1b)$$

where S_{n-1} and S_n are the vectors of the S_i-state population before and after the nth flash of the train, Y_n is the oxygen yield due to the nth flash, and $[S_2]_{n-1}$ and $[S_3]_{n-1}$ are the population of the redox states S_2 and S_3 before the nth flash. In the most generalized form, the S vectors contain also the formal redox states "S_{-1}" and "S_{-2}". Likewise, the transition matrix K comprises the univalent redox transitions "S_{-2}" → "S_{-1}" and "S_{-1}" → S_0, i.e.

$$[S]_n = \begin{bmatrix} ["S_{-2}"] \\ ["S_{-1}"] \\ [S_0] \\ [S_1] \\ [S_2] \\ [S_3] \end{bmatrix}_n \quad \text{and} \quad \mathbf{K} = \begin{bmatrix} \alpha & 0 & 0 & 0 & 0 & 0 \\ \gamma & \alpha & 0 & 0 & 0 & 0 \\ \beta & \gamma & \alpha & 0 & \beta & \gamma \\ 0 & \beta & \gamma & \alpha & 0 & \beta \\ 0 & 0 & \beta & \gamma & \alpha & 0 \\ 0 & 0 & 0 & \beta & \gamma & \alpha \end{bmatrix} \quad (2)$$

where $\gamma = 1 - \alpha - \beta$. The parameters of misses (α) and double hits (β) are assumed to be the same for all S states.

The computer program minimizes the expression

$$\sum_n (y_n^f - y_n^{exp})^2 \quad (3)$$

by three parameters in one run. In eq 3 $y_n^f = Y_n^f / \sum Y_n^f$ and $y_n^{exp} = Y_n^{exp} / \sum Y_n^{exp}$ represent the normalized values of the oxygen yield of the nth flash of the fitted (f) and experimental (exp) data. In all runs, Kok parameters were free in the range of $0 \le \alpha \le 0.4$, $0 \le \beta \le 0.33$, and $0 \le [S_i]_0 \le 1$, where $[S_i]_0$ is the population probability of redox state i before the first flash. The other initial state populations $[S_j]_0$ with $j \neq i$ were fixed in a trial and error method. Several runs were performed to adjust normalized populations of more than one special state S_i. The normalization criterion is given by

$$\sum_{i=-2}^{3} [S_i] = 1$$

Alternatively, the data fit was performed with an iterative method chosing the variation parameters $[S_i]_0$, α, and β by trial and error. In some cases, the possible formation of an additional formal redox state "S_{-3}" was considered.

Results

Oscillation Patterns of Oxygen Yield in Absence and Presence of NH_2OH or NH_2NH_2. Figure 2 shows typical oscillation patterns of the oxygen yield as a function of the flash number in dark-adapted thylakoids in the absence and presence of either 250 μM NH_2OH or 1 mM NH_2NH_2. The top traces were obtained with control samples in redox state $Y_D^{ox}S_1$ (circles) or with thylakoids containing an enriched S_0 population generated by the preillumination with three saturating flashes and subsequent incubation in the dark (20 min) before excitation with the flash train (triangles). Incubation of $Y_D^{ox}S_1$ thylakoids with 1 mM NH_2NH_2 in the dark for 20 min leads to a two-digit phase shift of the oscillation pattern (circles in the middle trace). This can be explained by the transformation of S_1 into a formal redox state "S_{-1}". If, however, a significant population of the S_0 state is achieved before NH_2NH_2 addition, a markedly different oscillation pattern is observed (triangles in the middle trace). This finding suggests that a state more reduced than the formal "S_{-1}" redox state can be generated by the interaction between NH_2NH_2 and PS II in the S_0 state. This reaction is assigned to the transition of S_0 into a formal redox state "S_{-2}" as proposed recently (Renger et al., 1990b; Messinger & Renger, 1990a). Accordingly, NH_2NH_2 can be considered as a reductant that generates a two-electron pool at the PS II donor side, regardless of the population ratio $[S_0(0)]/[S_1(0)]$ at NH_2NH_2 incubation time $t = 0$.

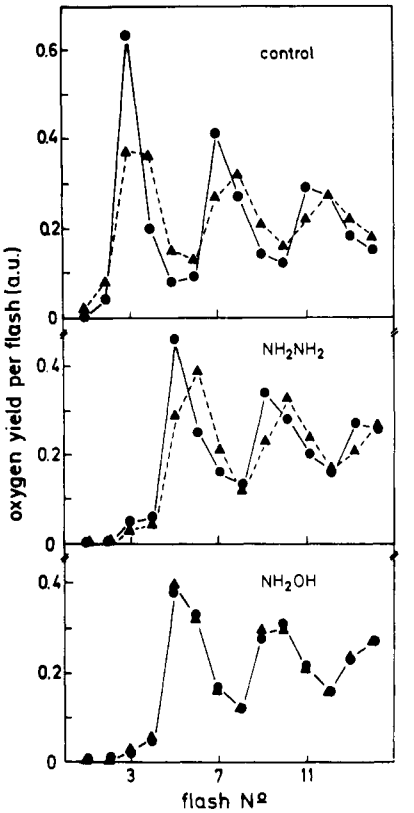

FIGURE 2: Oxygen yield per flash as a function of flash number in dark-adapted thylakoids. All samples were preilluminated by one preflash followed by a 1-h dark incubation on ice. (Top) Control samples preilluminated without (circles) or with (triangles) three additional preflashes and a 20-min dark incubation on ice before the measurement. (Middle) Injection of NH_2NH_2 into thylakoid suspensions pretreated by illumination without (circles) or with (triangles) three additional flashes and subsequent dark adaptation. The measurements were performed 20 min after NH_2NH_2 addition (final concentration in the suspension was 1 mM). (Bottom) Same experiment as in the middle part, but in the presence of 250 μM NH_2OH instead of 1 mM NH_2NH_2. Measurements were performed 5 min after NH_2OH addition.

A different phenomenon is observed if analogous experiments are performed with 250 μM NH_2OH instead of 1 mM NH_2NH_2. In this case, the oscillation patterns are almost independent of $[S_0(0)]/[S_1(0)]$ in the sample before addition of NH_2OH as shown by the traces in the bottom part of Figure 2.

The above results and earlier comparative studies (Hanssum & Renger, 1985) seem to indicate that NH_2OH and NH_2NH_2 interact with PS II via different reaction mechanisms. In order to address this problem in more detail, the time courses of the underlying processes were analyzed. Oxygen yields due to the 3rd, 4th, 5th, and 6th flash of the train symbolized by Y_3, Y_4, Y_5, and Y_6, respectively, were measured as a function of dark incubation time at 0 °C in the presence of either 50 μM NH_2OH or 1 mM NH_2NH_2 at pH 7.2. On the left side of Figure 3 the results are depicted for $Y_D^{ox}S_1$ (top) and S_0-enriched (bottom) thylakoids before NH_2OH addition. These data show that after 15 min the levels of Y_3 to Y_6 attain similar values in both samples, in general correspondence with the results shown in Figure 2 (bottom). However, the transient time courses in Figure 3 (left side) exhibit remarkable differences. The most pronounced effect is observed for Y_4. In $Y_D^{ox}S_1$ thylakoids, short-time incubation with NH_2OH leads to a transient maximum, while Y_4 declines steadily from $t =$

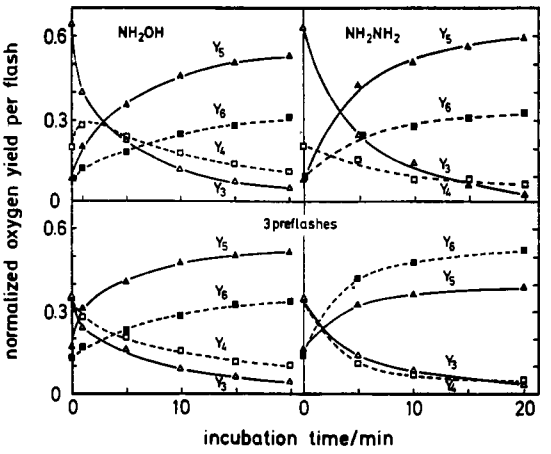

FIGURE 3: Normalized oxygen yield of the nth flash, Y_n, as a function of the total incubation time between addition of either NH_2OH (final concentration 50 μM) or NH_2NH_2 (final concentration 1 mM) and the actinic flash train in $Y_D^{ox}S_1$ thylakoids (top traces) or samples enriched in S_0 by three preflashes and subsequent dark incubation (bottom traces). For experimental details, see Materials and Methods.

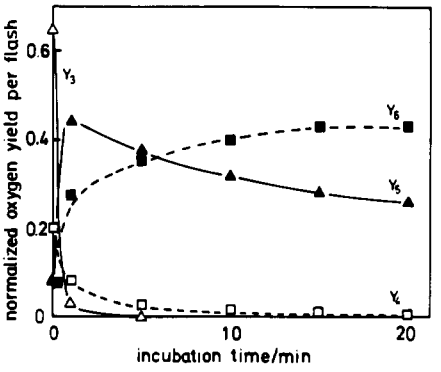

FIGURE 4: Normalized oxygen yield of the nth flash, Y_n, as a function of the total incubation time between addition of NH_2OH (final concentration 250 μM) and the actinic flash train in $Y_D^{ox}S_1$ thylakoids. For experimental details, see Materials and Methods.

0 in the S_0-enriched sample with increasing incubation times. This phenomenon can be explained by a NH_2OH-induced one-electron reduction mechanism:

$$S_1 \xrightarrow{k_{(NH_2OH)}(S_1)} S_0 \xrightarrow{k_{(NH_2OH)}(S_0)} \text{“}S_{-1}\text{”} \qquad (4)$$

Figure 3 (right side) reveals a different behavior with NH_2NH_2 as reductant. In this case, the Y_3 to Y_6 values in samples incubated for 15 min with 1 mM NH_2NH_2 exhibit a strong dependence on the initial S_0 and S_1 population before NH_2NH_2 addition (compare top and bottom traces). A closer inspection of the data suggests that the reaction pattern is dominated by a two-electron mechanism of the type

$$S_1 \xrightarrow{k_{(NH_2NH_2)}(S_1)} \text{“}S_{-1}\text{”} \quad \text{and} \quad S_0 \xrightarrow{k_{(NH_2NH_2)}(S_0)} \text{“}S_{-2}\text{”} \qquad (5)$$

The existence of a formal redox state “S_{-2}” raises the question whether this state could be also achieved with NH_2OH as exogenous reductant. To check this idea, experiments were performed at a higher NH_2OH concentration. Figure 4 presents the values of Y_3 to Y_6 as a function of the dark incubation time of $Y_D^{ox}S_1$ thylakoids with 250 μM NH_2OH. In this case, the rate constants are markedly larger for the decay of Y_3 and the increase of Y_5 and Y_6, while the transient rise of Y_4 cannot be observed at the time resolution of our method (about 1 min, see Materials and Methods). The most interesting phenomenon, however, is the decline of Y_5 after having reached its maximum at about 1 min. The decay of Y_5 is accompanied by an increase of Y_6. Both phenomena

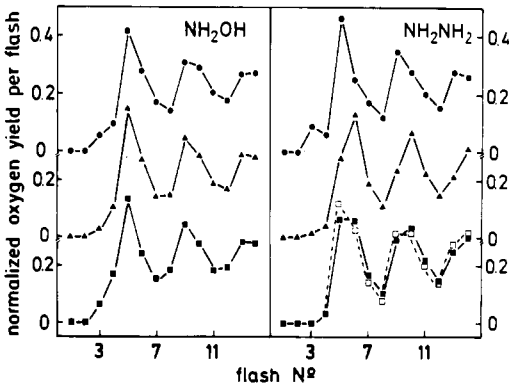

FIGURE 5: Oxygen yield per flash as a function of flash number in dark-adapted thylakoid suspensions in the presence of either 50 μM NH_2OH (left side) or 1 mM NH_2NH_2 (right side). For experimental details, see Materials and Methods and the text.

exhibit practically the same time course. This finding can be interpreted to reflect a slow univalent transformation of the formal redox state “S_{-1}” into that of “S_{-2}”. An analogous transient behavior of Y_5 and a concomitant rise of Y_6, inversely related to the Y_5 decay, is observed if the NH_2OH concentration is increased at an incubation time kept constant at 1 min [data not shown, the results correspond with those obtained previously by Hanssum and Renger (1985)].

As an alternative to the “S_{-2}” formation the decrease of the Y_5/Y_6 ratio in Figure 3 might be due to an elevated probability of misses, caused possibly by an interaction of NH_2OH with the PS II acceptor side (Renger et al., 1986; Sivaraja & Dismukes, 1988) and/or an accelerated S_2/S_3 decay between the flashes (Hanssum & Renger, 1985). As an example, the marked decrease of the Y_3/Y_4 ratio in PS II membrane fragments at high pH is rather due to an increase of misses than to an increase of the S_0/S_1 ratio (Renger & Hanssum, 1988). However, a detailed analysis of the data in NH_2OH treated thylakoids strongly supports the idea of “S_{-2}” formation also in NH_2OH-treated samples (see Discussion). Therefore, eq 4 can be extended by the reaction

$$\text{“}S_{-1}\text{”} \xrightarrow{k_{NH_2OH}(\text{“}S_{-1}\text{”})} \text{“}S_{-2}\text{”}. \qquad (4a)$$

For a further illustration of the differences between NH_2OH and NH_2NH_2, the following experiments were performed: $Y_D^{ox}S_1$ thylakoids were incubated on ice for 15 min in the dark with either 50 μM NH_2OH or 1 mM NH_2NH_2. The oxygen yield patterns obtained from a part of each sample are depicted at the top of Figure 5. They confirm that a high “S_{-1}” population is achieved with both substances. The remaining part of each sample was then illuminated with one saturating flash to oxidize “S_{-1}” into S_0. If NH_2OH and NH_2NH_2 interact with the newly formed S_0 state via a one-electron and two-electron donation, respectively, then the formal redox states “S_{-1}” and “S_{-2}” should be formed and, therefore, the oscillation patterns are anticipated to reveal marked differences. The results obtained with an aliquot of this sample are shown in the center part of Figure 5. The pattern observed in the NH_2OH sample is almost the same as that of the “S_{-1}” control sample, while in the case of NH_2NH_2 the maximum is clearly shifted to the 6th flash. The latter finding indicates that NH_2NH_2 predominantly reacts with S_0 under “S_{-2}” formation as suggested by eq 4. Illumination of the remaining sample with another flash should then again lead to the generation of the formal redox state “S_{-1}”, which is already achieved by incubation of control $Y_D^{ox}S_1$ thylakoids with NH_2NH_2. Accordingly, an oscillation pattern should be observed similar to that of Figure 5 (top, right side). Although

the results obtained (see Figure 5, bottom, right side) deviate due to the effect of misses inherently connected with each flash excitation, it can be clearly seen that after 10 min the O_2 yield of the 5th flash (Y_5) markedly exceeds that of the 6th flash (Y_6) as expected for a sample with a high "S_{-1}" state population (open squares). Even 45 min after the flash excitation the Y_5/Y_6 ratio markedly exceeds that of the "S_0" sample incubated for only 10 min (Figure 5, bottom, right side, closed squares). This confirms the idea that NH_2NH_2 mainly acts as a two-electron reductant for the PS II donor side. The data also show that "S_{-1}" can be further transformed by NH_2NH_2 (into "S_{-2}" or an even more reduced state "S_{-3}") via a very slow reaction. As anticipated, in the presence of NH_2OH, no significant differences are observed after illumination with an additional flash and subsequent dark adaptation (Figure 5, bottom, left side), because in this case the system always undergoes predominantly univalent oxidation (by the flash) and reduction (by NH_2OH) steps between "S_{-1}" and S_0. Slight deviations in the patterns at the left side of Figure 5 are mainly caused by the misses in each preillumination flash.

The results of Figures 3–5 strongly support the idea that NH_2OH and NH_2NH_2 are characterized by quite a different reduction mechanism: NH_2OH predominantly interferes with the PS II donor side as a univalent reductant, while NH_2NH_2 mainly acts as two-electron redox component. If one accepts this hypothesis, the effect observed with NH_2OH requires additional boundary conditions for the rate constants of the univalent redox steps:

$$k_{NH_2OH}(S_0) \gtrsim k_{NH_2OH}(S_1) \gg k_{NH_2OH}(\text{"}S_{-1}\text{"}) \qquad (6)$$

Determination of the Rate Constants of S_0 and S_1 Decay. The data reported so far do not provide information on the rate constants of the different processes. To address this point, the time course of the population probabilities of the redox states S_1, S_0, "S_{-1}", and "S_{-2}" were calculated by a numerical fit with eqs 1a,b–3 of experimental data analogous to those depicted in Figure 3. A rather simple behavior should arise, if $Y_D^{ox}S_1$ thylakoids are incubated in the dark with NH_2NH_2, because practically all PS II centers are in the redox state S_1 at $t = 0$. Therefore, only a transition into "S_{-1}" is expected to occur. A numerical fit confirms that the experimental data are satisfactorily described by a single two-electron transfer reaction with a rate constant of $k_{NH_2NH_2}(S_1) = 0.15$ min^{-1} at 0 °C and 1 mM NH_2NH_2.

A more complex pattern is expected if redox state S_0 is enriched in the sample by three preillumination flashes, followed by sufficient dark adaptation before addition of NH_2NH_2. The S_0 population achieved by this procedure is calculated to be about 65%. Accordingly, after completion of the reaction with NH_2NH_2, a population of 35% "S_{-1}" (from S_1) and 65% of "S_{-2}" is expected. The data obtained are in good agreement with this estimation. The pseudo-first-order rate constant of the reaction $S_0 \rightarrow$ "S_{-2}" induced by 1 mM NH_2NH_2 is calculated to be $k_{NH_2NH_2}(S_0) \approx 0.35$ min^{-1}. This value indicates that the reaction of NH_2NH_2 with the PS II donor side, with HSU(Mn) in redox state S_0, is about twice as fast as in the case of S_1.

This kinetic analysis confirms the hypothesis that NH_2NH_2 predominantly acts as a two-electron reductant of the PS II donor side. On the other hand, a markedly different reactivity pattern is observed with NH_2OH. First, it was found that at 50, 100, or even 150 μM NH_2OH the S_1-state population does not exhibit a pseudo-first-order decay but nicely fits a second-order kinetics (data not shown). This behavior (it will not be further analyzed in this study) could be a consequence of the interaction of NH_2OH with other target sites [e.g., the PS II acceptor side, see Renger et al. (1986) and Sivaraja and Dismukes (1988)]. Figure 6 depicts the time courses of the normalized population of the redox states S_1, S_0, "S_{-1}", and "S_{-2}" calculated by numerical fitting of the oscillation patterns measured at different dark incubation times after addition of 50 μM NH_2OH. Under these conditions, the pseudo-first-order approximation can provide only a qualitative description of the data (marked deviations arise especially at longer incubation times). In Figure 6 (top) $Y_D^{ox}S_1$ thylakoids were used. The data show that, in contrast to what is observed in the presence of 1 mM NH_2NH_2, a transient formation of S_0 takes place. The results also confirm that the NH_2OH-induced univalent reduction of S_1 into S_0 is slower than the subsequent transformation of S_0 into the formal redox state "S_{-1}". On the other hand, at 50 μM NH_2OH, the "S_{-1}" state is comparatively stable in the observed time domain to further univalent electron donation, giving rise to the formal redox state "S_{-2}".

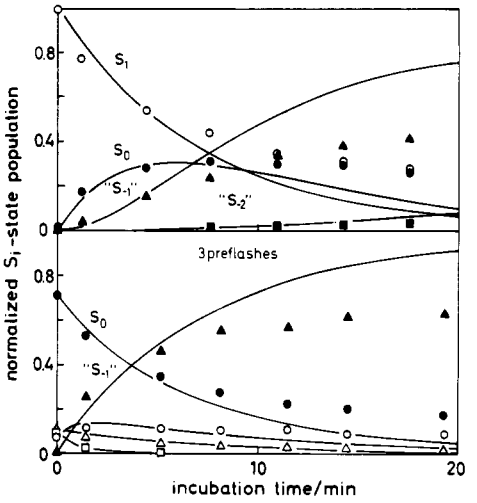

FIGURE 6: Normalized S_i-state population as a function of incubation time with 50 μM NH_2OH in dark-adapted thylakoids on ice. Experimental conditions and calculations as described under Materials and Methods. The theoretical curves were obtained according to eqs 4 and 4a (see text) with the apparent first-order rate constants $k_{NH_2OH}(S_1) = 0.16$ min^{-1}, $k_{NH_2OH}(S_0) = 0.20$ min^{-1}, and $k_{NH_2OH}(\text{"}S_{-1}\text{"}) \approx 0.01$ min^{-1}. Symbols: △, [S_3]; □, [S_2]; ○, [S_1]; ●, [S_0]; ▲, ["S_{-1}"]; and ■, ["S_{-2}"].

Table I: Average Values of the Rate Constants for Reactions of NH_2R with the Water Oxidase in Different Redox States, S_i, As Determined by Two (Three) Independent Methods

redox state	rate constant (M^{-1} s^{-1}) $k^0_{NH_2OH}(S_i)$	$k^0_{NH_2NH}(S_i)$	$k^0_{NH_2OH}/k^0_{NH_2NH_2}$
S_0	120 ± 20	8 ± 2	≈15
S_1	76 ± 10	4.3 ± 0.5	≈18
S_2	550 ± 100	33 ± 10	≈16
S_3	40 ± 10	1.7 ± 0.3	≈23

Figure 6 (bottom) shows the results obtained in thylakoids enriched with S_0 by three preflashes and a subsequent dark time (10 s) before incubation with 50 μM NH_2OH. On the basis of the first-order approximation, the following rate constants can be determined from Figure 6: $k_{NH_2OH}(S_1) \approx 0.16$ min^{-1}, $k_{NH_2OH}(S_0) \approx 0.20$ min^{-1}, and $k_{NH_2OH}(\text{"}S_{-1}\text{"}) \approx 0.01$ min^{-1}.

In order to confirm these data by another approach, measurements were performed of the corresponding S_i-state population as a function of the NH_2OH concentration at a constant reaction time of 1 min. The results obtained are depicted in Figure 7. The second-order rate constants, $k^0_{NH_2OH}(S_i)$, calculated from these curves are summarized in Table I.

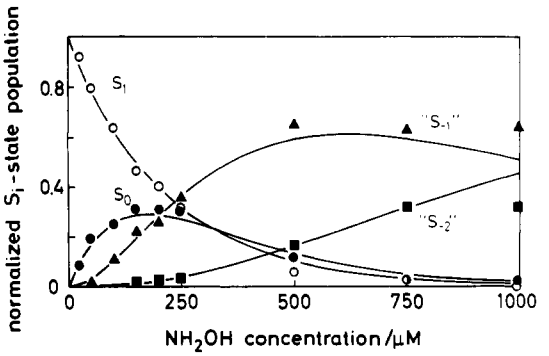

FIGURE 7: Normalized S_i-state population as a function of NH_2OH concentration at constant incubation time of 1 min on ice in dark-adapted thylakoids attaining state $Y_D^{ox}S_1$ at $t = 0$. Calculations of the S_i-state population and experimental details as described under Materials and Methods. The curves were calculated on the basis of a pseudo-first-order approximation with the following constants: $k^0_{NH_2OH}(S_1) = 76\ M^{-1}\ s^{-1}$, $k^0_{NH_2OH}(S_0) = 120\ M^{-1}\ s^{-1}$, and $k^0_{NH_2OH}("S_{-1}") \approx 17\ M^{-1}\ s^{-1}$.

These rate constants correspond with the values gathered from the measured time dependence at 50 μM NH_2OH.

Determination of the Rate Constants of S_2 and S_3 Decay. The analysis of the reactivities of NH_2OH and NH_2NH_2 at sufficiently low concentration (more complex patterns arising at higher concentrations will be outlined in a forthcoming paper), with the PS II donor side in the redox states S_1 and S_0 of HSU(Mn), raises the question on the mode of interaction with S_2 and S_3. Recently, both agents were found to exhibit a rather high reactivity toward S_2 compared with the surprisingly sluggish interaction with S_3 (Frank & Schmid, 1989; Messinger & Renger, 1990a). In order to address this problem in more detail, comparative studies were performed on the kinetics and the reaction mechanism (univalent versus bivalent redox reactions) of the NH_2OH- and NH_2NH_2-induced decay of S_2 and S_3. To prevent interference with the fast univalent reduction processes by Y_D as endogenous electron donor, all experiments were performed with $Y_D^{ox}S_1$ thylakoids (Messinger & Renger, 1990a). Formation of S_2 and S_3 by illumination of $Y_D^{ox}S_1$ thylakoids with one and two flashes, respectively, was immediately followed by addition of either 50 μM NH_2OH or 1 mM NH_2NH_2. After the desired dark incubation on ice, the samples were rapidly transferred to the Joliot-type electrode, and the oscillation patterns of the oxygen yield were measured as described under Materials and Methods. In order to distract the effects induced by the exogenous reductants, the experimental data obtained in the presence of either NH_2OH or NH_2NH_2 were corrected for the decay process caused by endogenous electron donors (S_2 and S_3 decay) or acceptors (S_0 oxidation to S_1, see Figure 1). The correction is based on the assumption that both reaction types are independent of each other [see Messinger and Renger (1990a)]. The most striking feature of these data [for further details, see Messinger and Renger (1990a)] is the very high susceptibility of the PS II donor side to both substances (NH_2OH, NH_2NH_2), if HSU(Mn) attains the redox state S_2, and the markedly diminished reactivity in S_3. The following rate constants were obtained: $k_{NH_2OH}(S_2) \geq 1.5\ min^{-1}$ and $k_{NH_2OH}(S_3) = 0.08\ min^{-1}$, $k_{NH_2NH_2}(S_2) \geq 1.8\ min^{-1}$, and $k_{NH_2NH_2}(S_3) \approx 0.05\ min^{-1}$. Two interesting phenomena emerge from these values: (i) both exogenous reductants give rise to decay rates of S_2 which exceed that of S_3 by more than one order of magnitude, and (ii) the concentrations required to achieve similar rate constants differ by a factor of about 20 for NH_2OH and NH_2NH_2, respectively (see Discussion and Table I).

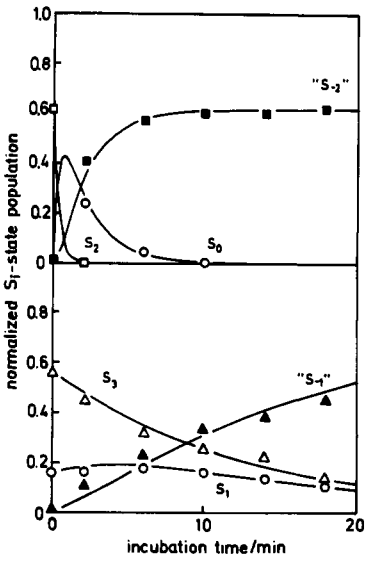

FIGURE 8: Normalized S_i-state population as a function of incubation time on ice with 1 mM NH_2NH_2 in thylakoids populated in S_2 (top) and S_3 (bottom) by one and two preflashes just before addition of NH_2NH_2. The S_i-state populations were calculated on the basis of eqs 7a and 7b with the apparent first-order rate constants $k_{NH_2NH_2}(S_2) = 2.8\ min^{-1}$ and $k_{NH_2NH_2}(S_0) = 0.5\ min^{-1}$ (curves at top part); $k_{NH_2NH_2}(S_3) = 0.08\ min^{-1}$ and $k_{NH_2NH_2}(S_1) = 0.17\ min^{-1}$ (curves at bottom part). For the sake of clarity the $S_1 \rightarrow$ "S_{-1}" (top) and the $S_2 \rightarrow S_0 \rightarrow$ "S_{-2}" (bottom) transitions are not shown.

Now, another interesting mechanistic problem will be addressed. In the previous sections, NH_2OH was inferred to act mainly as a one-electron reductant, while NH_2NH_2 reacts predominantly via two-electron redox reactions with either S_0 or S_1. Therefore, an analogous difference could also exist for the mechanism of reductive S_2 and S_3 decay. To address this point, the oscillation patterns used for the calculation of S_2 and S_3 decay were deconvoluted into the normalized S_i state population by using eqs 1a,b–3 and a fit program as described under Materials and Methods. The analysis of the data obtained with NH_2NH_2 according to

$$S_2 \xrightarrow{k_{NH_2NH_2}(S_2)} S_0 \xrightarrow{k_{NH_2NH_2}(S_0)} "S_{-2}" \qquad (7a)$$

$$S_3 \xrightarrow{k_{NH_2NH_2}(S_3)} S_1 \xrightarrow{k_{NH_2NH_2}(S_1)} "S_{-1}" \qquad (7b)$$

is complicated by the fact that we could never achieve an initial S_2 or S_3 state population of 100% by our flashing regime due to the intrinsic Kok parameters. The results obtained are depicted in Figure 8. The top traces show the values of $[S_2(t)]$, $[S_0(t)]$, and ["S_{-2}"(t)] calculated by the deconvolution analysis of data measured in samples with an initial S_2-state population, $[S_2(0)]$, of about 60%. Unfortunately, the fast decay of S_2 cannot be monitored due to the limited time resolution of our assay [see Messinger and Renger (1990a)]. The fit of the data for $[S_0(t)]$ and ["S_{-2}"(t)] is consistent with the reaction sequence of eq 7a giving rate constants of $k_{NH_2NH_2}(S_2) \approx 2.8\ min^{-1}$ and $k_{NH_2NH_2}(S_0) \approx 0.5\ min^{-1}$. The $k_{NH_2NH_2}(S_0)$ value is in good agreement with the corresponding rate constant ($0.35\ min^{-1}$) gathered from the numerical fit of measurements in samples enriched with S_0 before NH_2NH_2 addition. A different pattern is observed for the reaction sequence of NH_2NH_2-induced decay of S_3, where the overall kinetics are limited by the rather slow S_3 decay and the time courses of $[S_i(t)]$ ($i = 3, 1, "-1"$) can be satisfactorily described by the reaction sequence in eq 7b. The values of $[S_3(t)]$, $[S_1(t)]$, and ["S_{-1}"(t)] derived from the deconvolution analysis are depicted in Figure 8 (bottom). The best fit is obtained with $k_{NH_2NH_2}(S_3) = 0.08\ min^{-1}$ and $k_{NH_2NH_2}(S_1) = 0.17\ min^{-1}$.

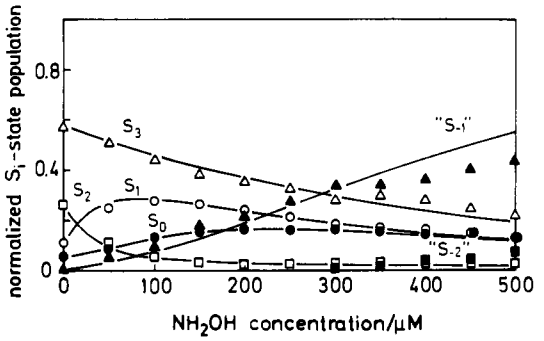

FIGURE 9: Normalized S_i-state population as a function of NH_2OH concentration at constant incubation time on ice for 1 min after addition of NH_2OH. The thylakoids were populated in S_3 by two preflashes just before addition of NH_2OH. The S_i-state populations were calculated as described under Materials and Methods. The curves were calculated on the basis of eq 8 with $k_{NH_2OH}(S_3) = 37\ M^{-1}\ s^{-1}$, $k_{NH_2OH}(S_2) = 470\ M^{-1}\ s^{-1}$, $k_{NH_2OH}(S_1) = 100\ M^{-1}\ s^{-1}$, and $k_{NH_2OH}(S_0) = 130\ M^{-1}\ s^{-1}$. Symbols: △, [$S_3$]; □, [$S_2$]; ○, [$S_1$]; ●, [$S_0$]; ▲, ["$S_{-1}$"]; and ■, ["$S_{-2}$"].

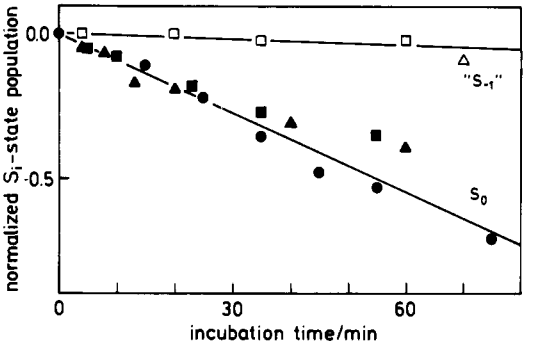

FIGURE 10: Semilogarithmic plot of the normalized population of "S_{-1}" and S_0 in NH_2OH (triangles) or NH_2NH_2 (squares) pretreated thylakoids without (open symbols) and with illumination with one flash (closed symbols) as a function of incubation time in NH_2R-free buffer on ice. For comparison the data of the S_0 population of the control treated with 3 preflashes are given (●). For details, see the text.

The latter value nicely fits the corresponding rate constant (0.15 min^{-1}) gathered from data obtained in $Y_D^{ox}S_1$ thylakoids, incubated in the dark with 1 mM NH_2NH_2. The rate constants of the NH_2NH_2-induced S_i decay were also determined by an independent method based on measurements as a function of NH_2NH_2 concentration at constant reaction time. From the results obtained (data not shown), second-order rate constants were obtained, which were compiled in Table I. A comparison of the data reveals that the two independent methods lead to results of good correspondence. In conclusion, the data presented here strongly support the idea that NH_2NH_2 interacts with the PS II donor side of spinach thylakoids predominantly via two-electron redox steps by reaction sequences described in eq 7a,b.

A different reaction mechanism is expected for the NH_2OH induced decay of S_2 and S_3. On the basis of the data of Figure 6, it appears likely that the reaction sequence is dominated by univalent redox steps as described by

$$S_3 \xrightarrow{k_{NH_2OH}(S_3)} S_2 \xrightarrow{k_{NH_2OH}(S_2)} S_1 \xrightarrow{k_{NH_2OH}(S_1)} S_0 \xrightarrow{k_{NH_2OH}(S_0)}$$
$$\text{"}S_{-1}\text{"} \xrightarrow{k_{NH_2OH}(\text{"}S_{-1}\text{"})} \text{"}S_{-2}\text{"} \quad (8)$$

The rate constants as determined by the concentration dependence of the S_i-state population at constant reaction time (Figure 9) give second-order rate constants, which are summarized in Table I. The results of Figures 6 and 9 also reveal that a synchronization of the water oxidase in "S_{-1}" can never be achieved with NH_2OH. Therefore, difference spectra obtained in the presence of NH_2OH (Saygin & Witt, 1987) have to be considered with precaution. Our data highly support recent conclusions of Lavergne (1989) concerning the problems related with NH_2OH.

In order to characterize further details of the reaction mechanism, the activation energy of the NH_2R-induced transformation of S_1 according to eqs 4 and 5 was determined by measurements of the rate constants as a function of temperature within the physiological range of 273 K < T < 293 K. An Arrhenius plot of the $k_{NH_2R}(S_1)$ values exhibits a parallel decline for the NH_2OH- and NH_2NH_2-induced S_1 decay characterized by an activation energy of about 50 kJ/mol (data not shown).

Another question of mechanistic relevance emerges from recent EPR studies (Sivaraja & Diskmukes, 1988), which revealed that Y_D^{ox} is not reduced by NH_2OH at concentrations sufficient for an $S_1 \rightarrow$ "S_{-1}" transition: What is the redox interaction between Y_D^{ox} and the water oxidase in the states S_0 and "S_{-1}"? To address this question, experiments were performed with thylakoids highly populated with "S_{-1}" by incubation with NH_2R. These samples were centrifuged and resuspended in NH_2R-free buffer solution. A part of each sample was then illuminated by one flash, leading to a high S_0 population. The NH_2R-free thylakoids in state S_0 and "S_{-1}" were incubated in the dark on ice for different times before the oscillation patterns were measured in aliquots of these samples. The S_i populations were calculated according to eqs 1a,b–3. All operations were performed in darkness to avoid any undesired "S_{-1}" oxidation. The results of [$S_0(t)$] and [$S_{-1}(t)$] are depicted in Figure 10 as a semilogarithmic plot. The data unequivocally show that "S_{-1}" in the Y_D^{ox}"S_{-1}" thylakoids remains practically unaffected during 1-h dark incubation at 0 °C; whereas in $Y_D^{ox}S_0$ thylakoids the S_0 state becomes slowly oxidized into S_1. This finding is very interesting because it shows that the "S_{-1}" state is much more resistant to oxidation by Y_D^{ox} than S_0.

Discussion

The present study was undertaken to further investigate the interaction of exogenous amine-type reductants NH_2R (R = OH or NH_2) with the reaction pattern of the water oxidase in intact thylakoids. In general, the following conclusions can be made: (a) the reaction mechanism of NH_2R exhibits remarkable differences, where NH_2OH acts predominantly as one-electron reductant, while NH_2NH_2 mainly functions as a two-electron reductant; (b) the activation energies, E_A, of the reduction processes in dark-adapted samples are very similar for both NH_2OH and NH_2NH_2, with the E_A values in the order of 50 kJ/mol over the physiological temperature range of 273 K < T < 293 K; (c) there exists convincing evidence for a formal redox state "S_{-2}"; (d) among the different redox states, S_0, ..., S_3, the most oxidized form, S_3, exhibits the slowest reduction rate with either NH_2OH or NH_2NH_2, while S_2 is the most reactive state.

In order to understand these results and their implications, it appears worthwhile to consider first a basic scheme for the reaction of NH_2R with the water oxidase and then to discuss the data within the framework of this scheme, taking into account current models for the mechanism of photosynthetic water oxidation.

Simplified Interaction Scheme of NH_2R with the Water Oxidase. In a generalized form the NH_2R-induced reduction pattern can be described by Scheme I. Here, {HSU(Mn)·X}$_i$ represents the water oxidase in redox state S_i consisting of a

Scheme I

$$\{HSU(Mn)\cdot X\}_i + NH_2R \underset{k_{-2}}{\overset{k_2}{\rightleftharpoons}} \{HSU(Mn)\cdot X\cdot NH_2R\}_i \xrightarrow{k_1} \{HSU(Mn)\cdot X\}_{i-r}$$
$$\searrow \text{products}$$

HSU(Mn) that is functionally connected with a site X within PS II. This site X directly interacts with NH_2R either as only redox inert binding site or as an electron acceptor via a redox active component referred to as C_{II}. So far C_{II} is not substantiated. It represents either a redox active protein component or transition metal groups (e.g., additional manganese) other than the presumed binuclear center of the catalytic site [see Renger and Wydrzynski (1991)]. An "irreversibly" bound NH_2R cannot be totally excluded (vide infra). $\{HSU(Mn)\cdot X\cdot NH_2R\}_i$ symbolizes the association complex between X and NH_2R of the water oxidase in state S_i, while $\{HSU(Mn)\cdot X\}_{i-r}$ represents the product of a dark reaction, where either component C_{II} in site X or directly the HSU(Mn) is reduced by $r = 1, 2$ electrons leading to a formal "S_{i-r}" state, with $r = 1$ or 2 for R = OH or NH_2, respectively; k_1, k_2, and k_{-2} are the rate constants of the corresponding reactions (in the special case of "irreversible" NH_2R binding, k_1 would represent the trapping process without product formation).

According to Scheme I the disappearance of redox state S_i due to NH_2R reduction is described as

$$d[S_i]_{total}/dt = -k_1[\{HSU(Mn)\cdot X\cdot NH_2R\}_i] \quad (9)$$

with

$$[S_i]_{total} = [\{HSU(Mn)\cdot X\}_i] + [\{HSU(Mn)\cdot X\cdot NH_2R\}_i] \quad (10)$$

A generalized analytical expression for $[S_i(t)]_{total}$ cannot be obtained, but two limiting cases will be discussed:

(A) k_2, $k_{-2} \gg k_1$, i.e., the intermediary state $\{HSU(Mn)\cdot X\cdot NH_2R\}_i$ always attains an equilibrium with S_i and NH_2R during the course of the reaction (except for a fast transient at the beginning). In this case eq 9 simplifies to

$$\frac{d[S_i]_{total}}{dt} = -k_1\frac{K_{eq}[NH_2R]}{1 + K_{eq}[NH_2R]}[S_i]_{total} \quad (11)$$

with $K_{eq} = k_2/k_{-2}$.

If $K_{eq}[NH_2R]$ is large, eq 11 leads to a monoexponential decay with a rate constant that is independent of $[NH_2R]$. As our results reveal an almost linear dependence of the rate constant on $[NH_2R]$, the value of K_{eq} cannot exceed 10^5 M^{-1} for NH_2OH in eq 11. A simple expression also derives under our experimental conditions $[NH_2OH] < 1$ mM for $K_{eq} < 10^2$ M^{-1}. Then we obtain from eq 11

$$\frac{d[S_i]_{total}}{dt} = -k_1K_{eq}[NH_2R][S_i]_{total} \quad (12)$$

In this case, the electron transfer from NH_2R to an endogenous redox group [either component C_{II} or HSU(Mn) (vide infra)] would be the rate-limiting step of the overall reaction.

(B) $k_2 \ll k_1$, i.e., the transient population $[\{HSU(Mn)\cdot X\cdot NH_2R\}_i]$ is always very low and the stationary state condition can be used, leading to

$$\frac{d[S_i]_{total}}{dt} = -\frac{k_2k_1}{k_{-2} + k_1}[NH_2R][S_i]_{total} \quad (13)$$

which formally gives the same concentration dependence as eq 12. In this case the binding of NH_2R to site X would be rate limiting. Therefore, any analysis based on an equation of the type

$$\frac{d[S_i]_{total}}{dt} = -k^0_{app}[NH_2R][S_i]_{total} \quad (14)$$

does not permit a decision on which reaction step is rate limiting.

In a previous study (Beck & Brudvig, 1988) only the former mechanism was discussed. However, the alternative case of $k_2 \ll k_1$ cannot be excluded, if site X is effectively shielded from rapid equilibration with the aqueous environment. Examples for very efficient shielding barriers of redox centers in PS II are well known, e.g., for Q_A^- to exogenous oxidants (Renger, 1976a,b) and for the strongly oxidizing Y_D^{ox} to exogenous reductants (Sivaraja & Dismukes, 1988; Vass et al., 1990b).

On the other hand, there is some evidence in favor of a fast equilibrium: (i) if the transport rate to site X is assumed to be similar for NH_2OH and NH_2NH_2, then the marked difference between the reductive efficiency of both species is indicative of a rate-limiting electron transfer step (symbolized by k_1); and (ii) a value of about 50 kJ/mol for the NH_2R-induced S_1 transformation into "S_{-1}" is very similar to that observed for S_2 and S_3 reduction by Y_D (Messinger & Renger, 1990b; Vass et al., 1990a) and the Q_A^- reoxidation by $Q_B(Q_B^-)$ (Gleiter et al., 1990). On the basis of these considerations, we favor a rate-limiting electron transfer, although an unambiguous answer cannot be achieved on the basis of our current knowledge.

Regardless of the above question, our data [lifetime of "S_{-1}" in NH_2R-free buffer (Figure 10) versus NH_2R-induced formation] clearly show that NH_2R undergoes a reaction that is irreversible within the time scale of these experiments. The most obvious explanation is the assumption of a dark reduction at or near the water oxidase. This idea is in line with our recent mass spectroscopic measurements on N_2 formation due to dark incubation of thylakoids with NH_2R (Renger et al., 1990b).

Mechanisms of Electron Donation to Water Oxidase by NH_2R. The NH_2R-induced reductive two-digit shift of the oxygen oscillation pattern is often attempted to synchronize the S_i-state population of the water oxidase in one definite redox state other than S_1 that is attained in sufficiently dark-adapted samples without NH_2R (Vermaas et al., 1984). Apart from the problems in achieving this goal (see results of Figures 6 and 7), it is mechanistically important to answer the question of whether NH_2R directly reduces the HSU(Mn) of the water oxidase or donates the electron(s) to an accessory two-electron pool (symbolized by C_{II}) at or near the NH_2R-binding site X. At first glance a direct reduction of the HSU(Mn) seems to provide the most simple way to interpret the kinetic data, which reveal that the rate constants of $S_i \rightarrow S_{i-r}$ transitions ($i = 0, 1, 2$; $r = 1, 2$) are practically the same regardless of the mode of generation of a particular S_i state (by preflashes and/or NH_2R incubation). However, the alternative idea of an intermediate electron carrier has to be considered for the following reasons: (a) it can explain the formal redox state "S_{-2}" (vide infra); (b) it is consistent with a previous proposal on the existence of an endogenous two-electron redox component in PS II that interacts with the S_i states (Lavorel & Maison-Peteri, 1983); (c) it fits nicely recent data which show that incubation of dark adapted samples (S_1 state) with NH_2OH does not affect the edge of X-ray absorption of the manganese cluster (Guiles et al., 1990a); (d) it explains the markedly longer lifetime of "S_{-1}" compared with that of S_0 (see Figure 10). In this case, the reduced form C_{II}^{red} could specifically interact as a one- or two-electron donor with S_2 and S_3 in an analogous way as the endogenous Y_D or the

exogenous ADRY agents (Hanssum et al., 1985). The electron transfer from C_{II}^{red} to S_2 and S_3 has then to be fast enough ($k > 5\ s^{-1}$) to account for the observed oscillation patterns. This idea is highly supported by findings of Förster and Junge (1988) indicating that a flash-induced formation of S_0 from "S_{-1}" is limited by a 30-ms kinetics. The possibility of a faster preceeding reaction (3 ms) giving rise to a H^+ release cannot be checked by the type of experiments performed in the present study. In Scheme I (comprising a further redox step), k_1 is then determined by the rate-limiting oxidation of NH_2R by C_{II} at site X.

Another striking phenomenon is the one-electron reductive pathway induced by NH_2OH versus the two-electron reactions with NH_2NH_2. The difference in the reductive pathways is probably due to the reactivity of the $^{\bullet}NHR$ radical (deprotonated form) formed by the first univalent oxidation step. It seems likely that the abstraction of the first electron occurs via a similar mechanism for both species, i.e., NH_2OH and NH_2NH_2. This idea is supported by the very similar activation energies of the S_1 decay, induced either by NH_2OH or NH_2NH_2. However, presumably for the $^{\bullet}NHNH_2$ radical the second electron is rapidly transferred to the redox-active group within the water oxidase [HSU(Mn) or component(s) C_{II} at site X], thereby giving rise to a two-electron reduction that is kinetically limited by the first electron abstraction. In contrast, NH_2OH does not act as two-electron donor. So far, no $^{\bullet}NHOH$ radicals could be detected (Förster & Junge, 1988). This observation can be easily explained by the assumption that the $^{\bullet}NHOH$ radical will be either internally trapped (e.g., by the protein) or it reacts with a second $^{\bullet}NHOH$ radical under N_2 formation. The dissipation of the $^{\bullet}NHOH$ is in all likelihood much faster than its very slow formation rate via the reaction sequence of Scheme I (see Table I), and therefore the maximum radical concentration remains below the detection limit. On the other hand, in Tris-treated samples selectively deprived of their oxygen evolution capacity, the oxidation by $P680^+$ or Y_z^{ox} is probably much faster, so that the formation of radicals like $(CH_3)_2NO^{\bullet}$ can be detected (Beck & Brudvig, 1987).

Previous measurements of the EPR multiline signal reflecting the redox state S_2 led to the conclusion that NH_2OH causes a two-electron reduction of S_1 into "S_{-1}" (Beck & Brudvig, 1988; Sivaraja & Dismukes, 1988). This is in line with our results which show that with NH_2OH up to 70% of the centers can attain the formal redox state "S_{-1}". Unfortunately the EPR measurements did not permit resolution of the sequence of the univalent redox step leading from S_1 to "S_{-1}" because the oscillation patterns were not measured as a function of incubation time. Another mechanistically interesting point is the possibility of cooperative reactions (Förster & Junge, 1985; Hanssum & Renger, 1985). Although an analysis of this problem is beyond the scope of the present study, our data unambiguously show that in the presence of NH_2OH no NH_2NH_2-type two-electron reduction is observed throughout a wide concentration range; i.e., the concerted reduction of two NH_2OH molecules within the same water oxidase appears to be very unlikely.

The Formal Redox State "S_{-2}". It has been suggested that the state "S_{-1}" represents the fully reduced binuclear manganese center of the water oxidase (Saygin & Witt, 1987). This idea, however, is difficult to reconcile with the much faster oxidation of S_0 by Y_D^{ox} than of "S_{-1}", if both states are ascribed to Mn(II)Mn(III) and Mn(II)Mn(II) for S_0 and "S_{-1}", respectively [see also Discussion in Renger et al. (1990b)]. Apart from this problem and the discrepancy with the X-ray data (Guiles et al., 1990a), the above proposal is in direct conflict with the existence of a redox state "S_{-2}", unless other redox centers [e.g., manganese of another dimeric unit or other redox-active ligands; for a discussion, see Renger and Govindjee (1985)] are assumed to be involved. The data of this study and of a previous communication (Renger et al., 1990b) provide strong support for the existence of a well-defined redox state "S_{-2}" based on the following reasons: (i) The detailed pattern of the two-digit phase shift induced by NH_2NH_2 depends unambiguously on the initial S_i state population (i = 0 or 1) before addition of the reductant. The difference persists during an incubation of 1 h, which leads to a significant decrease of the total oxygen-evolution capacity (Renger et al., 1990b). (ii) NH_2NH_2 leads to an almost quantitative transformation of S_0 directly into "S_{-2}", regardless of the mode for achieving a high S_0 population [either by three perflashes or by NH_2NH_2-induced S_2 decay (this study)]. (iii) A satisfactory fit of the oscillation patterns caused by NH_2OH treatment at higher concentrations and/or longer incubation times cannot be achieved without assuming the existence of "S_{-2}" (a change of the Kok parameters α and β can account for the decrease of Y_5/Y_6 but does not properly describe the whole oscillation pattern). On the basis of these data, it is very clear that "S_{-1}" is not the most reduced "stable" state of the water oxidase. However, it has to be emphasized that the formation of "S_{-2}" by NH_2OH (starting from S_1) requires either a direct reduction of S_1 to S_0, e.g., during the "S_{-1}" → "S_{-2}" transition, or the existence of two C_{II} components. This could be in line with the observation of a minor extend (up to 25%) of "S_{-3}" after longer incubation times with NH_2NH_2.

Implications of the Reactivity Order toward NH_2R-Induced Reduction of the Water Oxidase in Different Redox States S_i. In correspondence with our recent communication (Messinger & Renger, 1990a), the present analysis reveals that the NH_2R-induced reduction of the water oxidase exhibits the following reactivity order:

$$k_{NH_2R}(S_0) > k_{NH_2R}(S_1) \ll k_{NH_2R}(S_2) \gg k_{NH_2R}(S_3)$$

The second-order rate constants obtained in the present study are summarized in Table I. In the literature, second-order rate constants are reported only for the NH_2OH-induced transformation of S_1. In isolated PS II membrane fragments from spinach, a value of $k^0_{NH_2OH}(S_1) = 45.6 \pm 10\ M^{-1}\ s^{-1}$ was obtained (Beck & Brudvig, 1988). Unfortunately, no pH value was given. Regardless of this uncertainty, our $k^0_{NH_2OH}(S_1)$ of $76 \pm 10\ M^{-1}\ s^{-1}$ in isolated spinach thylakoids is in good correspondence. This indicates that the transport rate of NH_2R across the thylakoid membrane does not kinetically affect its interaction with the water oxidase. Furthermore, the accessibility of the water oxidase to exogenous reductants is not markedly affected by the detergent (Triton X-100) treatment used for the isolation of the PS II membrane fragments. This idea is in line with previous findings for NH_2OH-induced S_2 decay in PS II membrane fragments [*a* second-order rate constant of $k^0_{NH_2OH} \approx 300\ M^{-1}\ s^{-1}$ can be estimated from the data of Andreasson and Hansson (1987)].

The far most interesting finding, however, is the unusual S_i state dependent order of reactivity. Table I shows that the water oxidase exhibits practically the same behavior toward NH_2OH and NH_2NH_2 despite the different mechanism (one-electron versus two-electron pathway) and higher (15–20-fold) reductive efficiency of NH_2OH compared to NH_2NH_2 (on the basis of total concentration). Therefore, the large difference between S_3 and S_2 has to be considered as a general property of the water oxidase reactivity toward redox-active amines of comparatively small molecular size. This

conclusion is supported by recent findings in etiolated oat chloroplasts (Franck & Schmid, 1989). It is remarkable that in contrast to the reaction pattern of these small molecules, secondary amines with bulky aromatic substituents like certain diphenylamines (Oettmeier & Renger, 1980) or anilinothiophenes (Renger, 1972) specifically reduce the lifetime of S_2 and S_3 with no significant reactivity difference between both redox states (Hanssum et al., 1985). This consideration clearly illustrates that the molecular architecture around the water oxidase plays a key role in the reactivity of the endogenous redox-active groups. It is currently widely accepted that the redox-active manganese cluster in S_3 either exhibits a lack of one electron compared with S_2 (Dekker et al., 1984; Saygin & Witt, 1987; Beck & Brudvig, 1987) or has the same redox state plus a singly oxidized ligand (Guiles et al., 1990b; Boussac et al., 1990a). In either of these hypotheses, the drastic decrease of reactivity between small redox-active amines, NH_2R, and the water oxidase in state S_3 compared with S_2, can be explained only by a significant structural change taking place during the $S_2 \rightarrow S_3$ transition. This modification has either to significantly reduce (see Table I) the accessibility of the presumed endogenous site X to NH_2R (i.e., $k_2 \ll k_1$, see eq 13) or to retard the electron transfer step from bound NH_2R to the acceptor (i.e., $k_2 \gg k_1$, see eq 12). The triggering of such a significant structural change by a single electron abstraction is not easily understood, if one compares the redox transitions $S_1 \rightarrow S_2$ and $S_2 \rightarrow S_3$. In the first case, according to EXAFS measurements no structural change is inferred to take place at the manganese cluster (Guiles et al., 1990b). Therefore, in the case of rate limitation by k_1, the marked increase of NH_2R reactivity in S_2 is directly or indirectly related to the higher manganese redox state. On the other hand, in either of the models a similar electron abstraction from S_2 has to give rise to a marked nuclear rearrangement in order to decrease the reactivity in S_3 toward NH_2R. Therefore, it appears attractive to consider an alternate interpretation. A structural change could take place as the consequence of an electronic redistribution between ligated substrate water and a functional binuclear manganese cluster, giving rise to formation of a complexed peroxide (Renger, 1978, 1987b). This reorganization of the electronic configuration and nuclear geometry could be responsible for the rather sluggish reaction of NH_2R in redox state S_3. It is often argued that a peroxide would spontaneously oxidize to O_2, leading to overreduction of the manganese center. Indeed, the water oxidase was shown to exhibit pseudo-catalase activity (Mano et al., 1987; Frasch & Mei, 1987). The above-mentioned argument, however, is only tenable for free peroxide. A complexed peroxide stabilized by about 100 kJ/mol (Renger, 1978) can behave totally different. Other arguments often raised against a peroxidic state in S_3 are based on the $H_2{}^{18}O$ experiments of Radmer and Ollinger (1986) and of Bader et al. (1987). However, as outlined in Renger (1987b), these experiments cannot provide an unambiguous answer due to the limited time resolution. It has to be emphasized that the concentration of water exceeds that of NH_2R by orders of magnitude. Therefore the rate of interaction with the water oxidase can be estimated to be faster than a few milliseconds provided that the second-order rate constants have comparable values for H_2O and NH_2R. In comparison to that, the time resolution of the above-mentioned isotope exchange experiments is in the order of 1 min.

The formation of a peroxidic species in S_3 could provide a suitable reaction pathway for oxidation of two H_2O molecules to O_2. The further abstraction of only one electron from this state in S_3 by $Y_Z{}^{ox}$ would trigger the simultaneous ejection of a second electron and fast release of O_2. This process can easily explain the fast kinetics of oxygen formation (Joliot & Kok, 1975; Lavergne, 1990; Strzalka et al., 1990).

The data of our study also show that the redox state S_2 is most susceptible to rapid reduction by small redox-active amines of the type NH_2R (R = OH, NH_2). This property is very likely related to the high sensitivity of water oxidase in redox state S_2 toward degradation by high pH (Frasch & Cheniae, 1980) or Tris-washing (Briantais et al., 1977) and the quite different interaction (mode and kinetics) of S_2 and S_3 with NH_3 (Velthuys, 1975; Boussac et al., 1990b).

On the basis of the results presented here and data taken from the literature, the redox state S_2 of the water oxidase is inferred to be already so susceptible to reductive decay that a further electron abstraction step without concomitant electronic and nuclear redistribution would lead to a very rapid degradation of the water oxidase. The mode of protection of the redox state S_3 remains to be clarified, but it is clearly reflected by the sluggish reaction with reductive NH_2R species.

The present study revealed that NH_2R compounds are a useful tool that provides very interesting information about the properties of the different redox states of the water oxidase.

ACKNOWLEDGMENTS

We thank Dr. T. Wydrzynski for critical reading of the manuscript and many helpful comments. We also thank S. Hohm-Veit for drawing the figures.

Registry No. NH_2OH, 7803-49-8; NH_2NH_2, 302-01-2; O_2, 7782-44-7; water oxidase, 114514-26-0.

REFERENCES

Andreasson, L.-E., & Hansson, Ö. (1987) in *Progress in Photosynthesis Research* (Biggens, J. Ed.) Vol. I, pp 503–510, Martinus Nijhoff Publishers, Dordrecht.

Babcock, G. T. (1987) in *New Comprehensive Biochemistry* (Amesz, J., Ed.) Vol. 15, Photosynthesis, pp 125–158, Elsevier, Amsterdam.

Bader, K. P., Thibault, P., & Schmid, G. H. (1987) *Biochim. Biophys. Acta 893*, 564–571.

Beck, W. F., & Brudvig, G. W. (1987) *Biochemistry 26*, 8285–8295.

Beck, W. F., & Brudvig, G. W. (1988) *J. Am. Chem. Soc. 110, 1517*–1523.

Bouges, B. (1971) *Biochim. Biophys. Acta 234*, 102–112.

Boussac, A., Zimmermann, J.-L., Rutherford, A. W., & Lavergne, J. (1990a) *Nature 347*, 303–306.

Boussac, A., Rutherford, A. W., & Styring, S. (1990b) *Biochemistry 29*, 24–32.

Briantais, J. M., Vernotte, C., Lavergne, J., & Arntzen, C. J. (1977) *Biochim. Biophys. Acta 461*, 61–74.

Debus, R. J., Barry, B. A., Sithole, I., Babcock, G. T., & McIntosh, L. (1988a) *Biochemistry 27*, 9071–9074.

Debus, R. J., Barry, B. A., Babcock, G. T., & McIntosh, L. (1988b) *Proc. Natl. Acad. Sci. U.S.A. 85*, 427–430.

Dekker, J. P., van Gorkom, H. J., Wensink, J., & Ouwehand, L. (1984) *Biochim. Biophys. Acta 767*, 1–9.

Förster, V., & Junge, W. (1985) *FEBS Lett. 186*, 153–157.

Förster, V., & Junge, W. (1988) *Chem. Scripta 28A*, 111–116.

Franck, F., & Schmid, G. H. (1989) *Biochim. Biophys. Acta 977*, 215–218.

Frasch, W. D., & Cheniae, G. M. (1980) *Plant Physiol. 65*, 735–745.

Frasch, W. D., & Mei, R. (1987) *Biochemistry 26*, 7321–7325.

Gleiter, H. M., Haag, E., & Renger, G. (1990) in *Current*

Research in Photosynthesis (Baltscheffsky, M., Ed.) Vol. I, pp 375–378, Kluwer, Dordrecht.
Guiles, R. D., Yachandra, V. K., McDermott, A. E., Cole, J. L., Dexheimer, S. L., Britt, R. D., Sauer, K., Klein, M. P. (1990a) *Biochemistry 29*, 486–496.
Guiles, R. D., Zimmermann, J.-L., McDermott, A. E., Yachandra, V. K., Cole, J. L., Dexheimer, S. L., Britt, R. D., Wieghardt, K., Bossek, U., Sauer, K., & Klein, M. P. (1990b) *Biochemistry 29*, 471–485.
Hansson, Ö., & Wydrzynski, T. (1990) *Photosynth. Res. 23*, 131–162.
Hanssum, B., & Renger, G. (1985) *Biochim. Biophys. Acta 810*, 225–234.
Hanssum, B., & Renger, G. (1987) in *Progress in Photosynthesis Research* (Biggins, J., Ed.) Vol. 1, pp 515–518, Martinus Nijhoff, Dordrecht.
Hanssum, B., Dohnt, G., & Renger, G. (1985) *Biochim. Biophys. Acta 806*, 210–220.
Joliot, P. (1972) *Methods Enzymol. 24*, 123–134.
Joliot, P., & Kok, B. (1975) in *Bioenergetics of Photosynthesis* (Govindjee, Ed.) pp 387–412, Academic Press, New York.
Kok, B., & Velthuys, B. R. (1977) in *Research in Photobiology* (Castellani, A., Ed.) pp 111–119, Plenum Press, New York.
Kok, B., Forbush, B., & McGloin, M. (1970) *Photochem. Photobiol. 11*, 457–475.
Lavergne, J. (1989) *Photochem. Photobiol. 50*, 235–241.
Lavergne, J. (1990) in *Current Research in Photosynthesis* (Baltscheffsky, M., Ed.) Vol. I, pp 893–896, Kluwer, Dordrecht.
Lavorel, J., & Maison-Peteri, B. (1983) *Physiol. Veg. 21*, 509–517.
Mano, J., Takahashi, M., & Asada, K. (1987) *Biochemistry 26*, 2495–2501.
Messinger, J., & Renger, G. (1990a) *FEBS Lett. 277*, 141–146.
Messinger, J., & Renger, G. (1990b) in *Current Research in Photosynthesis* (Baltscheffsky, M., Ed.) Vol. I, pp 849–852, Kluwer, Dordrecht.
Metz, J. G., Nixon, P. J., Rögner, M., Brudvig, G. W., & Diner, B. A. (1989) *Biochemistry 28*, 6960–6969.
Oettmeier, W., & Renger, G. (1980) *Biochim. Biophys. Acta 593*, 113–124.
Radmer, R., & Ollinger, O. (1986) *FEBS Lett. 195*, 285–289.
Renger, G. (1972) *Biochim. Biophys. Acta 256*, 428–439.
Renger, G. (1976a) *Biochim. Biophys. Acta 440*, 287–300.
Renger, G. (1976b) *FEBS Lett. 69*, 225–230.
Renger, G. (1978) in *Photosynthetic Water Oxidation* (H. Metzner, Ed.) pp 229–248, Academic Press, London.
Renger, G. (1987a) *Angew. Chem., Int. Ed. Engl. 26*, 643–660.
Renger, G. (1987b) *Photosynthetica 21*, 203–224.
Renger, G., & Govindjee (1985) *Photosynth. Res. 6*, 33–35.
Renger, G., & Hanssum, B. (1988) *Photosynth. Res. 16*, 243–259.
Renger, G., & Wydrzynski, T. (1991) *Biol. Metals 4*, 73–80.
Renger, G., Hagemann, R., & Fromme, R. (1986) *FEBS Lett. 203*, 210–214.
Renger, G., Eckert, H.-J., & Völker, M. (1989) *Photosynth. Res. 22*, 247–256.
Renger, G., Bader, K. P., & Schmid, G. H. (1990a) *Biochim. Biophys. Acta 1015*, 288–294.
Renger, G., Messinger, J., & Hanssum, B. (1990b) in *Current Research in Photosynthesis* (Baltscheffsky, M., Ed.) Vol. 1, pp 845–848, Kluwer, Dordrecht.
Rutherford, A. W. (1989) *Trends Biochem. Sci. 14*, 227–232.
Rutherford, A. W., & Inoue, Y. (1983) *FEBS Lett. 165*, 163–170.
Rutherford, A. W., Renger, G., Koike, H., & Inoue, Y. (1984) *Biochim. Biophys. Acta 767*, 548–556.
Saygin, Ö., & Witt, H. T. (1987) *Biochim. Biophys. Acta 893*, 452–469.
Sivaraja, M., & Dismukes, G. C. (1988) *Biochemistry 27*, 3467–3475.
Strzalka, K., Walczak, T., Sarna, T., & Swartz, H. M. (1990) *Arch. Biochem. Biophys. 281*, 312–318.
Styring, S., & Rutherford, A. W. (1988) *Biochim. Biophys. Acta 933*, 378–387.
Vass, I., Deák, Z., & Hideg, E. (1990a) *Biochim. Biophys. Acta 1017*, 63–69.
Vass, I., Deák, Z., Jegerschöld, C., & Styring, S. (1990b) *Biochim. Biophys. Acta 1018*, 41–46.
Velthuys, B. R. (1975) *Biochim. Biophys. Acta 396*, 392–401.
Vermaas, W. F. J., Renger, G., & Dohnt, G. (1984) *Biochim. Biophys. Acta 764*, 194–202.
Vermaas, W. F. J., Rutherford, A. W., & Hansson, Ö. (1988) *Proc. Natl. Acad. Sci. U.S.A. 85*, 8477–8480.
Winget, G. H., Izawa, S., & Good, N. E. (1965) *Biochem. Biophys. Res. Commun. 21*, 438–441.
Wydrzynski, T., Huggins, B. J., & Jursinic, P. A. (1985) *Biochim. Biophys. Acta 809*, 125–136.